Proton Storage

Deutsche Ausgabe: DOI: 10.1002/ange.201507008
Internationale Ausgabe: DOI: 10.1002/anie.201507008

Remote Multiproton Storage within a Pyrrolide-Pincer-Type Ligand

*Soufiane S. Nadif, Matthew E. O'Reilly, Ion Ghiviriga, Khalil A. Abboud, and Adam S. Veige**

Abstract: *A chemically non-innocent pyrrole-based trianionic $(ONO)^{3-}$ pincer ligand within [(pyr-ONO)TiCl(thf)$_2$] (**2**) can access the dianionic [(3H-pyr-ONO)TiCl$_2$(thf)] (**1-THF**) and monoanionic [(3H,4H-pyr-ONO)TiCl$_2$(OEt$_2$)][B{3,5-(CF$_3$)$_2$C$_6$H$_3$}$_4$] (**3-Et$_2$O**) states through remote protonation of the pyrrole γ-C π-bonds. The homoleptic [(3H-pyr-ONO)$_2$Zr] (**4**) was synthesized and characterized by X-ray diffraction and NMR spectroscopy in solution. The protonation of **4** by [H(OEt$_2$)$_2$][B{C$_6$H$_3$(CF$_3$)$_2$}$_4$] yields [(3H,4H-pyr-ONO)(3H-pyr-ONO)Zr][B{3,5-(CF$_3$)$_2$C$_6$H$_3$}$_4$] (**5**), thus demonstrating the storage of three protons.*

It is well-understood that transporting liquid fuels[1] is more efficient and safer than the mass transport of gases.[2] Acids (formic)[3] and alcohols (methanol)[4] are potential media for storing dihydrogen (H_2)[5] produced by artificial leaf technologies.[6] Fujita and co-workers demonstrated the reversible storage of H_2 as formic acid by employing CO_2 and an iridium catalyst.[7] Grützmacher and co-workers demonstrated the storage and release of H_2 within methanol.[8] In both cases, a chemically non-innocent ligand receives protons before storing them as formic acid or methanol. Multiproton-responsive ligands[9] are emerging in other important transformations.[10] Umehara, Kuwata, and Ikariya demonstrated cleavage of the N–N bond of hydrazines with an Fe pincer complex that relies on the ability of the ligand to undergo redox changes through multiple reversible protonation events.[11] Thompson and Berben demonstrated the electrocatalytic production of dihydrogen by a ligand-based protonation approach.[12] Relatedly, Kirchner and co-workers demonstrated the heterolytic cleavage of dihydrogen with an Fe-NNN pincer complex.[13] In the Ru-PNP pincer[14] and the related PNN pincer developed by Milstein and co-workers,[15] a proton-transfer event within the backbone of the ligand is critical in the catalytic conversion of alcohols into esters and dihydrogen, and the hydrogenation of secondary amides, respectively. van der Vlugt, de Bruin, and co-workers presented rhodium pincer complexes capable of dynamic ligand reactivity.[16] A key feature within these examples is that the proton storage occurs at remote locations within the ligand, rather than on an atom adjacent to the metal center.

Similar to chemically non-innocent ligands, more conventional redox-active ligands are proving to be exceptionally capable of mediating multielectron transformations, a necessity to avoid uncontrollable and nonselective single-electron radical chemistry.[17] In particular and most relevant, Heyduk and co-workers introduced an ONO pincer ligand that shuttles from a trianionic pincer form $(ONO)^{3-}$, to its one electron oxidized dianionic radical form $(ONO)^{2-}$ (semiquinone), to its two electron oxidized monoanionic form $(ONO)^{-}$ (quinone; Figure 1 top).[18] Instead of shuttling

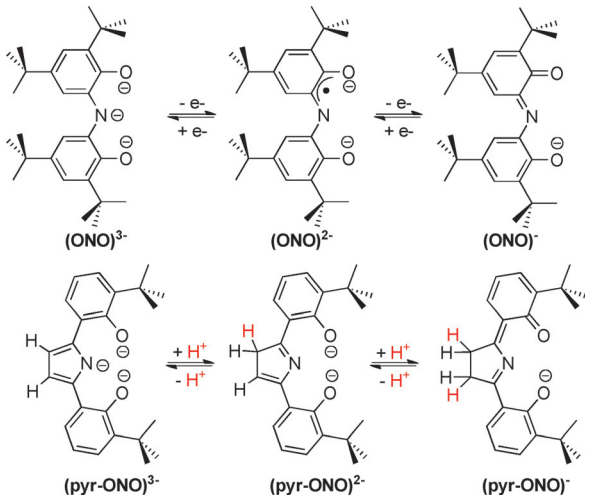

Figure 1. Comparison between a multielectron non-innocent ONO pincer ligand and a multiproton non-innocent ONO pincer ligand.

electrons, we now present a chemically non-innocent pincer ligand (pyr-ONO) that undergoes multiple reversible protonation events (Figure 1 bottom). An important criterion is that the protonation events occur remotely (i.e. the atom directly attached to the metal ion isn't simply protonated). Remote protonation of the pyrrolide converts the trianionic[19] ONO pincer ligand $(pyr\text{-}ONO)^{3-}$ into the dianionic form $(pyr\text{-}ONO)^{2-}$, and then a second protonation site on the pyrrolide enables access to the monoanionic form $(pyr\text{-}ONO)^{-}$. We can now access and characterize complexes exhibiting each state of the (pyr-ONO) ligand. To demonstrate the utility of the (pyr-ONO) ligand, we present a case which has the potential to store four protons within a single complex.

Treating a colorless solution of (pyr-ONO)H$_3$ in CH_2Cl_2 with [TiCl$_4$(thf)$_2$] results in an immediate color change to deep red. Evaporation of all the volatiles affords the dichloro complex [(*3H*-pyr-ONO)TiCl$_2$(thf)] (**1-THF**) as an analytically pure brown powder in 84% yield (Figure 2). Slow evaporation of a concentrated solution of **1-THF** in dichloromethane yields red crystals suitable for single-crystal X-ray diffraction. Figure 3 depicts the solid-state structure of **1-**

[*] S. S. Nadif, Dr. M. E. O'Reilly, Dr. I. Ghiviriga, Dr. K. A. Abboud, Prof. A. S. Veige
University of Florida, Center for Catalysis
P.O. Box 117200 (USA)
E-mail: veige@chem.ufl.edu
Homepage: https://veige.chem.ufl.edu/

Supporting information for this article is available on the WWW under http://dx.doi.org/10.1002/anie.201507008.

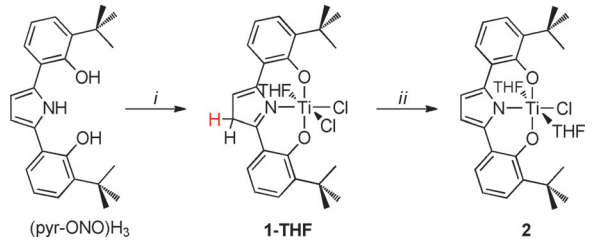

Figure 2. Synthesis of dianionic [(3*H*-pyr-ONO)$TiCl_2$(thf)] (**1-THF**) and trianionic [(pyr-ONO)Ti$(thf)_2$Cl] (**2**). Reaction conditions: i) [$TiCl_4$-$(thf)_2$], CH_2Cl_2, ii) 2,6-lutidine, CH_2Cl_2.

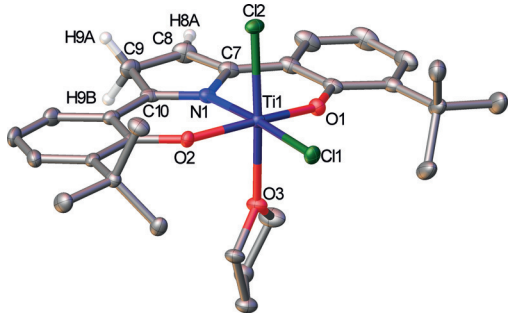

Figure 3. Molecular structure of **1-THF** with dichloromethane and all hydrogen atoms, except H9A, H9B, and H8A, removed for clarity.

THF. The C_1-symmetric complex contains a Ti^{IV} ion in a distorted octahedral geometry. The ligand is clearly in the dianionic state: protons H8A, H9A, and H9B were found in the difference Fourier map and refined freely to give C–H bond lengths of 0.93(3), 0.93(3), and 1.02(3) Å, respectively. Moreover, the asymmetry within the pyrrole moiety manifests in a short N1=C10 bond length of 1.332(3) Å, compared to the adjacent long N1–C7 bond length of 1.437(3) Å. Additionally, alternating long single (1.476(3) Å) and short C–C double bonds (1.358(3) Å) are observed within the pyrrole ring (Figure 4).

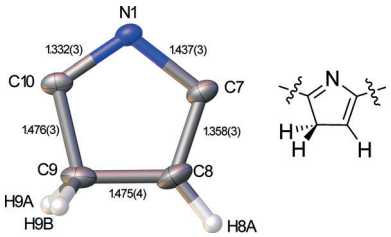

Figure 4. Truncated molecular structure focusing on the pyrrole ring within **1-THF** (bond lengths in Å).

A search of the Cambridge structural database[20] does not reveal any 3*H*-pyrrole ligands bound to a titanium center. Only a few examples of complexes with metal coordination to 3*H*-pyrrole protons are known, including the tungsten *N*-methyl, 3*H*-pyrrole complexes reported by Harman and coworkers[21] that bind the pyrrole ring through C=C η^2-coordination, a binding mode impossible within our pincer framework.

The ^{1}H NMR spectrum (C_6D_6) of **1-THF** exhibits pyrrole -CH_2- and -C=CH- resonances at 4.12 and 6.78 ppm, respectively, and two separate *t*Bu signals at 1.65 and 1.68 ppm. Distinguishing ^{13}C NMR signals include a resonance at 176.6 ppm for the imine carbon atom (N=C) and the olefinic carbon atoms that appear upfield at 151.0 (N–*C*=CH) and 115.4 ppm (N–C=*C*H). The most relevant finding from the ^{1}H NOESY NMR spectroscopic characterization is that all the protons are in dynamic exchange as a consequence of the methylene proton migrating from the 3- to the 4-position.

The addition of 2,6-lutidine to complex **1-THF** in CH_2Cl_2 removes the proton from the 3-position to provide the trianionic $(ONO)^{3-}$ state of the ligand. Complex **2**, after drying under vacuum, was purified by repeatedly adding Et_2O to a concentrated THF solution to precipitate 2,6-lutidinium chloride. A combination of ^{1}H NMR spectroscopy and gHMBC provides the absolute NMR assignments for the proton and carbon atoms in **2**. In the ^{1}H NMR spectrum of complex **2**, signals attributable to two symmetry-equivalent THF ligands and only one resonance at 1.87 ppm for the *t*Bu protons are consistent with the assigned C_{2v} symmetry (Figure 2). Indicative of an aromatic pyrrolide moiety, the signals for the CH protons in **2** shift downfield relative to those of **1-THF** into the aromatic region at 7.49 ppm, and their corresponding carbon atoms resonate at 109.3 ppm.

Effective proton storage requires facile addition and removal. Storing protons in the form of C–H bonds is an interesting approach; however, the newly formed C–H bond must give up the proton selectively and reversibly: remarkably, the pyrrole pincer ligand does both. Conducting the metalation of (pyr-ONO)H_3 with $TiCl_4$ in the absence of coordinating thf molecules provides complexes **1** and **3-Cl** in an equilibrium ratio of 87:13, respectively (Figure 5). The HCl generated in the metalation step must add to complex **1** in situ to form complex **3-Cl**. This does not occur when [$TiCl_4(thf)_2$]

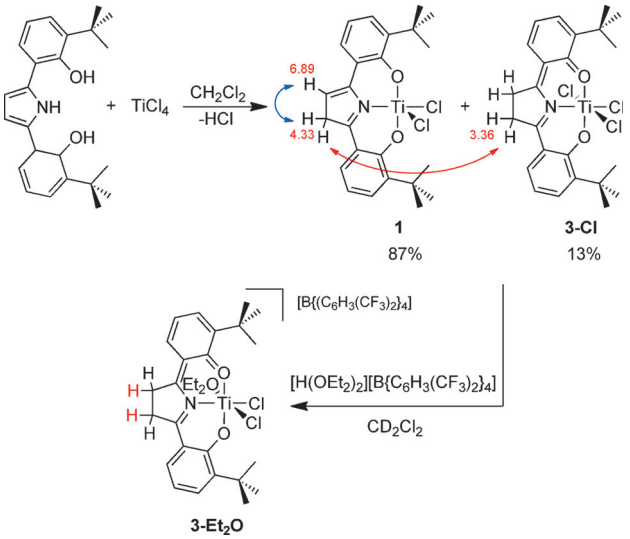

Figure 5. Preparation of a mixture of **1** and **3-Cl** and illustration of the dynamic reversible proton exchange between all C-H sites within the pyrrole ring and preparation of monanionic [(3*H*,4*H*-pyr-ONO)$TiCl_2$-(OEt_2)][B{3,5-$(CF_3)_2C_6H_3$}$_4$] (**3-Et$_2$O**). Selected ^{1}H NMR chemical shifts are shown in red.

is the metal substrate because the coordinated thf prevents the addition of HCl. Similar to **1-THF**, the C3 (4.33 ppm) and C4 protons (6.89 ppm) in **1** self-exchange. ^{1}H NOESY NMR spectroscopy with selective inversion at 4.33 ppm exhibits spin transfer polarization with the =CH− proton at 6.89 ppm. Moreover, demonstrating reversible storage, in solution, the C3 protons (4.33 ppm) on **1** and the C3/C4 protons (3.36 ppm) on **3-Cl** are also in rapid exchange (Figure 5).

Adding $[H(OEt_2)_2][B\{3,5\text{-}(CF_3)_2C_6H_3\}_4]$ to the mixture of complexes **1** and **3-Cl** in CD_2Cl_2 affords a single product featuring the monoanionic pincer state of the ligand in the complex $[(3H,4H\text{-pyr-ONO})TiCl_2(Et_2O)][B\{3,5\text{-}(CF_3)_2C_6H_3\}_4]$ (**3-OEt$_2$**) in situ (Figure 5). Complex **3-OEt$_2$** is stable in solution, but degrades upon further manipulations. Figure 6

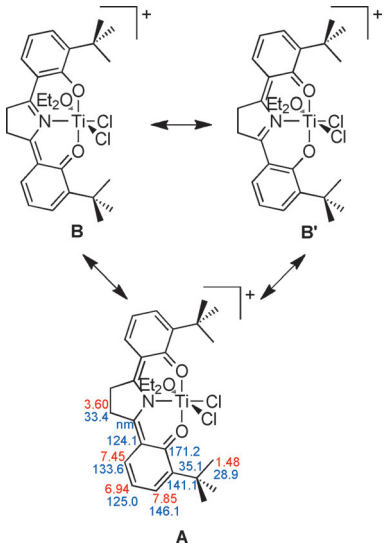

Figure 6. Three possible resonance forms for the monoanionic $(ONO)^-$ pincer ligand in **3-OEt$_2$**. Selected ^{1}H NMR chemical shifts are shown in red and ^{13}C NMR chemical shifts in blue.

depicts three resonance contributors that are plausible for complex **3-OEt$_2$**. In resonance form **A**, the N-atom carries the negative charge, whereas in the two degenerate resonance structures **B** and **B′** the negative charge resides on the oxygen atoms. Reflecting the three resonance contributors, the computed electronic structure contains molecular orbitals delocalized over the nine-atom π-system. All the orbitals (see Figure S53 in the Supporting Information) are consistent with **A**, **B**, and **B′**, and do not provide any distinguishing features. Each heteroatom bears some negative charge, but for simplicity the resonance contributor that places the negative charge on the more electronegative oxygen atom is presented.

Solid-state characterization in the form of a crystal structure of **3-Et$_2$O** was not possible due to challenges with stability and isolation. A combination of ^{1}H, ^{1}H-^{13}C gHSQC, and ^{1}H-^{13}C gHMBC NMR techniques provide data that enable the absolute assignment of the proton and carbon atoms within **3-OEt$_2$**. Consistent with the proposal that all the resonance forms contribute to the electronic structure, only one set of resonances are observed in the NMR spectra (see Figure 6 for NMR assignments). In contrast, the complex prepared by Heyduk and co-workers $[(ONO)TaCl_4]$ displays two distinct ^{13}C NMR resonances for the C=O and C–O moieties.[18a]

DFT geometry optimization of complex **1-THF** reproduces well the solid-state bond lengths and angles (see the Supporting Information). As complex **1-THF** was computed with good accuracy, geometry optimizations were also performed on complexes **2** and **3-OEt$_2$**. Figure 7 depicts truncated molecular orbital diagrams for complexes **1-THF**, **2**, and **3-Et$_2$O**. Examining their electronic structures provides a rational explanation for the ability of the (pyr-ONO) ligand to store two protons. Starting with the trianionic ligand in complex **2**, the HOMO orbital contains significant electron density on the pyrrolide C3- and C4-positions. Protonation of one of these positions provides the dianionic form in **1-THF**. Appropriately, the HOMO orbital in **1-THF** contains signifi-

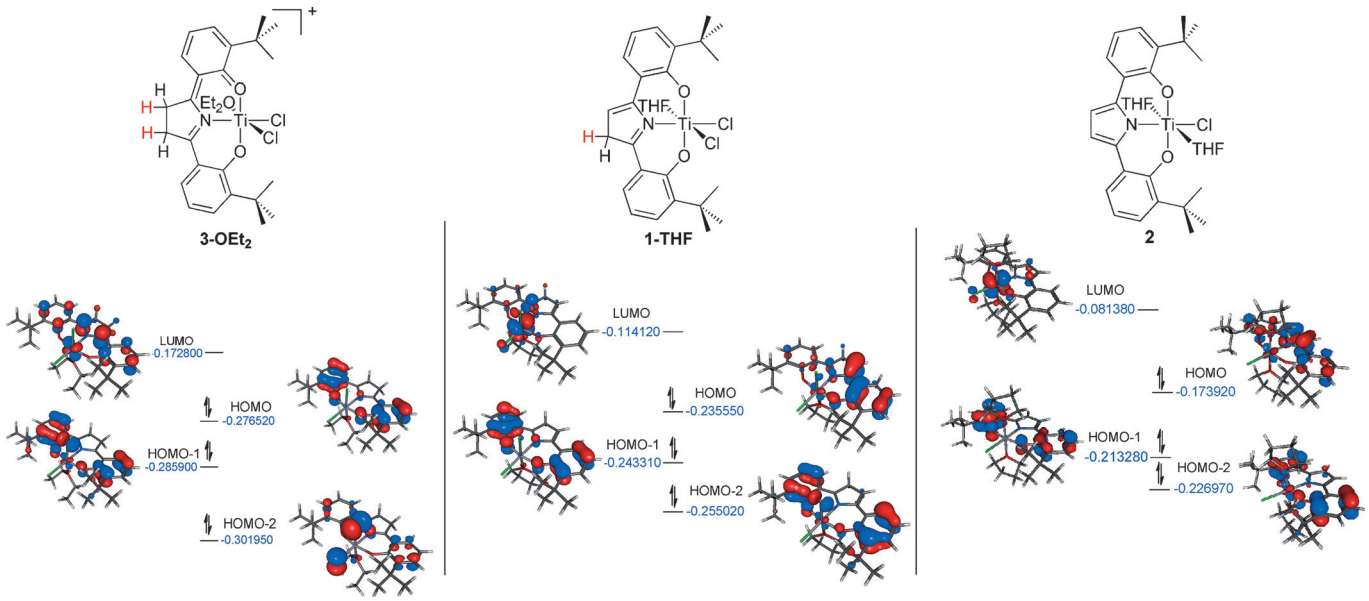

Figure 7. Truncated molecular orbital diagrams of **1-THF**, **2**, and **3-OEt$_2$** (isovalue = 0.044278).

cant electron density in the C4-position, thus protonation occurs there exclusively to provide the monoanionic ligand state in **3-OEt$_2$**. The HOMO orbital in **3-OEt$_2$** does not offer a reasonable site for additional protonation on the pincer framework, thus two protons are controllably stored.

Previous studies employing an $(OCO)^{3-}$ ligand showed that using homoleptic metal-alkyl compounds as opposed to metal halides as the metal substrates leads to double ligation.[22] In an attempt to build a complex capable of reversibly storing four protons, treating (pyr-ONO)H$_3$ with $ZrBn_4$ in benzene provides, as anticipated, the homoleptic complex [(3*H*-pyr-ONO)$_2$Zr] (**4**) as an analytically pure crystalline powder (Figure 8). An X-ray diffraction experiment performed on single crystals of **4** confirms its structural assignment (Figure 9). The complex has C_1 symmetry with the zirconium ion in a distorted octahedral geometry created by two perpendicular ligands in their dianionic state. The zirconium–nitrogen distances are 2.321(17) and 2.3440(19) Å, values similar to those in a 2*H*-pyrrole (2.315(2) Å) coordinated to a zirconium ion reported by Nocera and co-workers.[23] Electron densities for protons H8, H9A, H9B, H32, H33A, and H33B were found in the difference Fourier map to provide conclusive evidence that the ligands are in the dianionic state. In addition, similar to **1-THF**, the C3 and C4 protons on the pyrrole ring of **4** are in dynamic exchange (see Figure S29). The synthesis of complex **4** provides a clue as to the source of the proton that eventually protonates the pyrrole backbone. Since toluene is the by-product of the metalation, it is unlikely that toluene acts as the proton source ($pK_a = 43$ in DMSO), therefore, the pyrrole N-H proton is the likely source of the proton.

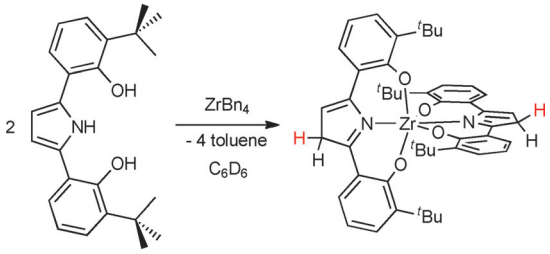

Figure 8. Synthesis of [(3*H*-pyr-ONO)$_2$Zr] (**4**).

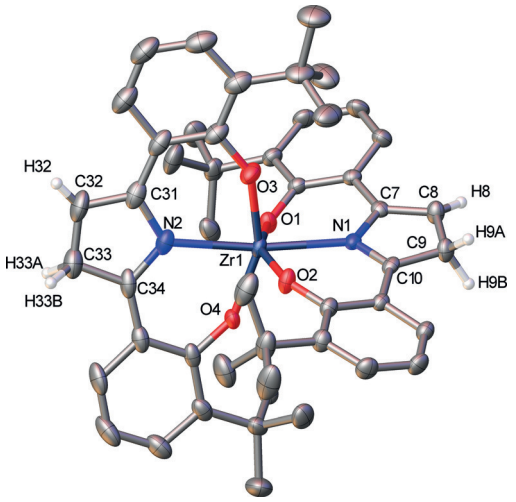

Figure 9. Molecular structure of **4**, with the calculated hydrogen atoms, *tert*-butyl groups, a lattice diethyl ether, and a lattice THF molecule removed for clarity.

To investigate the possibility of storing four protons per metal center, 2.1 equivalents of $[H(OEt_2)_2][B\{C_6H_3(CF_3)_2\}_4]$ were added to **4** in $CDCl_3$. This resulted in an immediate color change from yellow to dark turquoise and the formation of copious precipitate (Figure 10). The ^{1}H NMR spectrum of the soluble material is consistent with complex **5**, which bears both a monoanionic and a dianionic pincer ligand. Two distinct resonances at 4.39 and 3.62 ppm integrate to two and four protons, respectively. From a gHMBC study, the two protons at 4.39 ppm are assigned to a methylene group coupled to a methine =C–H at 6.88 ppm (see Figure 10). Attempts to isolate complex **5** were not successful. Over time, the insoluble material dissolves and the proton signals grow in the NMR spectrum, thus suggesting the initial precipitate is also **5**. The addition of more acid equivalents does not result in protonation of the fourth site. Compound **5** decomposes readily upon solvent evaporation, thus isolation was not successful; however, a combination of NMR techniques provides its absolute assignment in solution.

In conclusion, examples of pincer ligands changing oxidation states through protonation of a nitrogen donor[24] or electrochemically[18,25] are relatively common. However, in the case of the pyrrole-centered pincer ligand (pyr-ONO), the switch from a monoanionic state to a trianionic state through reversible remote protonation is unique. The only other related system is Milstein's PNP pincer that shuttles between a monoanionic and a neutral ligand by a single proton transfer event,[14] thus making (pyr-ONO) particularly distinguished and exciting because it offers the opportunity to shuttle two protons over three ligand states. Combining two (pyr-ONO)

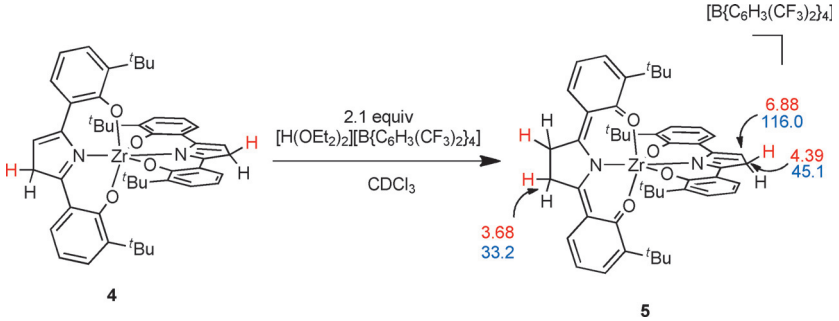

Figure 10. Preparation of the monoanionic/dianionic pincer complex **5** [(3*H*,4*H*-pyr-ONO)(3*H*-pyr-ONO)Zr][B{3,5-(CF$_3$)$_2$C$_6$H$_3$}$_4$]. Selected ^{1}H NMR chemical shifts are shown in red and ^{13}C NMR chemical shifts in blue.

ligands within one metal coordination sphere in complex **4** and its protonation to **5** demonstrates, for the first time, a pincer ligand complex that can remotely store a total of three protons, with the potential to store four.

Acknowledgements

A.S.V. acknowledges UF for providing funding for this research. This material is based upon work supported by the National Science Foundation CHE-1265993. K.A.A. acknowledges the NSF (CHE-0821346) for the purchase of X-ray equipment.

Keywords: N,O ligands · proton storage · protonation · redox chemistry · titanium

How to cite: *Angew. Chem. Int. Ed.* **2015**, *54*, 15138–15142
Angew. Chem. **2015**, *127*, 15353–15357

[1] H. L. Jiang, S. K. Singh, J. M. Yan, X. B. Zhang, Q. Xu, *ChemSusChem* **2010**, *3*, 541 – 549.
[2] R. K. Ahluwalia, T. Q. Hua, J. K. Peng, *Int. J. Hydrogen Energy* **2012**, *37*, 2891 – 2910.
[3] M. Grasemann, G. Laurenczy, *Energy Environ. Sci.* **2012**, *5*, 8171 – 8181.
[4] G. A. Olah, *Angew. Chem. Int. Ed.* **2005**, *44*, 2636 – 2639; *Angew. Chem.* **2005**, *117*, 2692 – 2696.
[5] T. C. Johnson, D. J. Morris, M. Wills, *Chem. Soc. Rev.* **2010**, *39*, 81 – 88.
[6] a) A. J. Bard, M. A. Fox, *Acc. Chem. Res.* **1995**, *28*, 141 – 145; b) D. G. Nocera, *Acc. Chem. Res.* **2012**, *45*, 767 – 776; c) Y. Tachibana, L. Vayssieres, J. R. Durrant, *Nat. Photonics* **2012**, *6*, 511 – 518; d) V. S. Thoi, Y. J. Sun, J. R. Long, C. J. Chang, *Chem. Soc. Rev.* **2013**, *42*, 2388 – 2400.
[7] a) J. F. Hull, Y. Himeda, W. H. Wang, B. Hashiguchi, R. Periana, D. J. Szalda, J. T. Muckerman, E. Fujita, *Nat. Chem.* **2012**, *4*, 383 – 388; b) W. H. Wang, J. F. Hull, J. T. Muckerman, E. Fujita, Y. Himeda, *Energy Environ. Sci.* **2012**, *5*, 7923 – 7926; c) W. H. Wang, J. F. Hull, J. T. Muckerman, E. Fujita, T. Hirose, Y. Himeda, *Chem. Eur. J.* **2012**, *18*, 9397 – 9404.
[8] R. E. Rodríguez-Lugo, M. Trincado, M. Vogt, F. Tewes, G. Santiso-Quinones, H. Grützmacher, *Nat. Chem.* **2013**, *5*, 342 – 347.
[9] a) S. Kuwata, T. Ikariya, *Chem. Commun.* **2014**, *50*, 14290 – 14300; b) R. Langer, I. Fuchs, M. Vogt, E. Balaraman, Y. Diskin-Posner, L. J. W. Shimon, Y. Ben-David, D. Milstein, *Chem. Eur. J.* **2013**, *19*, 3407 – 3414; c) M. Vogt, O. Rivada-Wheelaghan, M. A. Iron, G. Leitus, Y. Diskin-Posner, L. J. W. Shimon, Y. Ben-David, D. Milstein, *Organometallics* **2013**, *32*, 300 – 308; d) T. Zell, R. Langer, M. A. Iron, L. Konstantinovski, L. J. W. Shimon, Y. Diskin-Posner, G. Leitus, E. Balaraman, Y. Ben-David, D. Milstein, *Inorg. Chem.* **2013**, *52*, 9636 – 9649; e) C. M. Moore, N. K. Szymczak, *Chem. Commun.* **2013**, *49*, 400 – 402.
[10] a) H. Grützmacher, *Angew. Chem. Int. Ed.* **2008**, *47*, 1814 – 1818; *Angew. Chem.* **2008**, *120*, 1838 – 1842; b) C. Gunanathan, D. Milstein, *Acc. Chem. Res.* **2011**, *44*, 588 – 602; c) H. Li, B. Zheng, K.-W. Huang, *Coord. Chem. Rev.* **2015**, *293 – 294*, 116 – 138.
[11] K. Umehara, S. Kuwata, T. Ikariya, *J. Am. Chem. Soc.* **2013**, *135*, 6754 – 6757.
[12] E. J. Thompson, L. A. Berben, *Angew. Chem. Int. Ed.* **2015**, *40*, 11642 – 11646; *Angew. Chem.* **2015**, *127*, 11808 – 11812.
[13] B. Bichler, C. Holzhacker, B. Stöger, M. Puchberger, L. F. Veiros, K. Kirchner, *Organometallics* **2013**, *32*, 4114 – 4121.
[14] J. Zhang, G. Leitus, Y. Ben-David, D. Milstein, *J. Am. Chem. Soc.* **2005**, *127*, 10840 – 10841.
[15] R. Barrios-Francisco, E. Balaraman, Y. Diskin-Posner, G. Leitus, L. J. W. Shimon, D. Milstein, *Organometallics* **2013**, *32*, 2973 – 2982.
[16] a) Z. Tang, E. Otten, J. N. H. Reek, J. I. van der Vlugt, B. de Bruin, *Chem. Eur. J.* **2015**, *21*, 12683 – 12693; b) L. S. Jongbloed, B. de Bruin, J. N. H. Reek, M. Lutz, J. I. van der Vlugt, *Chem. Eur. J.* **2015**, *21*, 7297 – 7305.
[17] a) V. Lyaskovskyy, B. de Bruin, *ACS Catal.* **2012**, *2*, 270 – 279; b) O. R. Luca, R. H. Crabtree, *Chem. Soc. Rev.* **2013**, *42*, 1440 – 1459; c) D. L. J. Broere, R. Plessius, J. I. van der Vlugt, *Chem. Soc. Rev.* **2015**, *44*, 6886 – 6915.
[18] a) R. A. Zarkesh, J. W. Ziller, A. F. Heyduk, *Angew. Chem. Int. Ed.* **2008**, *47*, 4715 – 4718; *Angew. Chem.* **2008**, *120*, 4793 – 4796; b) A. F. Heyduk, R. A. Zarkesh, A. I. Nguyen, *Inorg. Chem.* **2011**, *50*, 9849 – 9863; c) S. Hananouchi, B. T. Krull, J. W. Ziller, F. Furche, A. F. Heyduk, *Dalton Trans.* **2014**, *43*, 17991 – 18000.
[19] M. E. O'Reilly, A. S. Veige, *Chem. Soc. Rev.* **2014**, *43*, 6325 – 6369.
[20] F. H. Allen, *Acta Crystallogr. Sect. B* **2002**, *58*, 380 – 388.
[21] W. H. Myers, K. D. Welch, P. M. Graham, A. Keller, M. Sabat, C. O. Trindle, W. D. Harman, *Organometallics* **2005**, *24*, 5267 – 5279.
[22] S. Kuppuswamy, I. Ghiviriga, K. A. Abboud, A. S. Veige, *Organometallics* **2010**, *29*, 6711 – 6722.
[23] J. Bachmann, T. S. Teets, D. G. Nocera, *Dalton Trans.* **2008**, 4549 – 4551.
[24] L. A. Berben, *Chem. Eur. J.* **2015**, *21*, 2734 – 2742.
[25] a) A. I. Nguyen, R. A. Zarkesh, D. C. Lacy, M. K. Thorson, A. F. Heyduk, *Chem. Sci.* **2011**, *2*, 166 – 169; b) R. F. Munhá, R. A. Zarkesh, A. F. Heyduk, *Dalton Trans.* **2013**, *42*, 3751 – 3766; c) J. L. Wong, R. H. Sanchez, J. G. Logan, R. A. Zarkesh, J. W. Ziller, A. F. Heyduk, *Chem. Sci.* **2013**, *4*, 1906 – 1910; d) A. I. Nguyen, K. J. Blackmore, S. M. Carter, R. A. Zarkesh, A. F. Heyduk, *J. Am. Chem. Soc.* **2009**, *131*, 3307 – 3316.

Received: July 28, 2015
Published online: October 22, 2015

